Annals of Botany **87**: 179–189, 2001
doi:10.1006/anbo.2000.1317, available online at http://www.idealibrary.com on IDEAL®

Ultrastructure of Early Secondary Embryogenesis by Multicellular and Unicellular Pathways in Cork Oak (*Quercus suber* L.)

PERE PUIGDERRAJOLS*, GISELA MIR and MARISA MOLINAS

Department de Biologia, Universitat de Girona, Laboratori del Suro, Campus Montilivi s/n., E-17071 Girona, Spain

Received: 10 July 2000 Returned for revision: 8 September 2000 Accepted: 2 October 2000 Published electronically: 18 December 2000

Early cellular events during secondary embryogenesis were studied in a cork oak recurrent embryogenic system in which embryos arise either in a multicellular budding pathway from a compact mass of proliferation or from isolated single cells in friable callus. The compact mass of proliferation originated from the epidermal cells at the hypocotyl whose growth and convolution was characterized by a decrease in the nucleus/cytoplasm ratio and a marked increase in storage products. The transition from the compact mass to meristematic primordia occurred at the periphery and was accompanied by cell dedifferentiation and a drastic reduction of storage products. Meristematic primordia evolved to globular embryos by the organization of a protodermis and two internal centres. Microscope analysis of friable callus showed an hypothetical sequence from single cells to aggregates of a few cells, meristematic cell clusters and globular embryos. Single cells showed typical features of embryogenic cells such as rich cytoplasm and a large number of starch grains and lipid bodies. A progressive cell dedifferentiation and a drastic reduction of storage products was observed when aggregates of a few cells and meristematic cell clusters were compared. Progressive bipolarization in large meristematic cell clusters initiated globular embryo formation. The comparison of both embryogenic pathways at the ultrastructural level showed that subcellular changes follow a similar sequential pattern, especially with regard to the storage products. The possible role of plastid extrusions and multivesicular bodies in the changing pattern of starch metabolism during embryogenesis is discussed. © 2001 Annals of Botany Company

Key words: *Quercus suber* L, cork oak, somatic embryogenesis, multicellular budding, friable callus, ultrastructural studies.

INTRODUCTION

Embryo production by recurrent or secondary embryogenesis is the step giving somatic embryogenesis a multiplicative potential for clonal mass propagation (Merkle, 1995). Secondary embryos arise from superficial single cells or by multicellular budding, usually at the hypocotyl of the mother embryo (Williams and Maheswaran, 1986). Embryo origin is especially relevant to the genetic uniformity of regenerated plants; as a multicellular origin may result in the formation of genetically variable chimeric plants, a unicellular origin is the desired pathway for practical applications of embryo cloning such as genetic transformation.

Recurrent systems are especially suited to the continuous production of friable callus, which is a valuable source of single cells with embryogenic capacity (Fransz and Schel, 1994). Nevertheless, information about embryos' actual origin and early differentiation in friable callus is scarce and fragmentary. In the literature most observers agree that embryos develop from small aggregates of embryogenic cells which, in turn, come from single cytoplasm-rich cells (Yeung, 1995). However, the whole developmental sequence from single cells to heart-shaped embryos has only been fully documented for the carrot suspension culture (Toonen *et al*., 1994; Yasuda *et al*., 2000). In addition, although ultrastructural characterization of friable callus may contribute greatly to a better understanding of the embryogenic process, subcellular studies have concentrated on carrot (Halperin and Jensen, 1967) and a few gramineous systems (Karlsson and Vasil, 1986; Fransz and Schel, 1991*a*, *b*; Taylor and Vasil, 1996). With regard to somatic embryogenesis from multiple cells, it has been described as taking place through a meristematic budding pattern, but only a few primary systems (Wernicke *et al*., 1982; McCain and Hodges, 1986; Stamp, 1987; Hepher *et al*., 1988; Schwendimann *et al*., 1988; Canhoto *et al*., 1996; Taylor and Vasil, 1996) and cork oak (*Quercus suber* L.) secondary embryogenesis (Puigderrajols *et al*., 1996) have been characterized morphologically. However, subcellular events have only been investigated in pearl millet (Gramineae) (Taylor and Vasil, 1996) and the woody pineapple guava (Myrtaceae) (Canhoto *et al*., 1996).

In the cork oak system, secondary embryos mainly originate by meristematic budding from a compact mass of proliferation (Puigderrajols *et al*., 1996, 2000). However, very occasionally, a brownish friable callus forms in areas of the hypocotyl in direct contact with the culture medium. Moreover, depending on culture conditions, a proliferating friable callus can be induced from which somatic embryos are easily isolated. Somatic embryogenesis by unicellular and multicellular pathways in the same explant has been demonstrated in cultured zygotic embryos of pearl millet (Taylor and Vasil, 1996) and pineapple guava (Canhoto *et al*., 1996). There is general agreement that, once the embryogenic process starts, there is no difference between

* For correspondence. Fax +34 972418150, e-mail dbppr@fe.udg.es

0305-7364/01/020179+11 $35.00/00 © 2001 Annals of Botany Company

single or multiple-cell origin, although evidence reported in the literature is scant and not always conclusive (Fransz and Schel, 1994). Therefore, further investigation is needed before this hypothesis can be confirmed. Embryogenic systems in which embryos develop along two pathways from the same explant may well be appropriate comparative models.

In the research reported in this paper, we investigated the ultrastructure of secondary embryo formation in a cork oak recurrent system. Our purpose was: (1) to define the

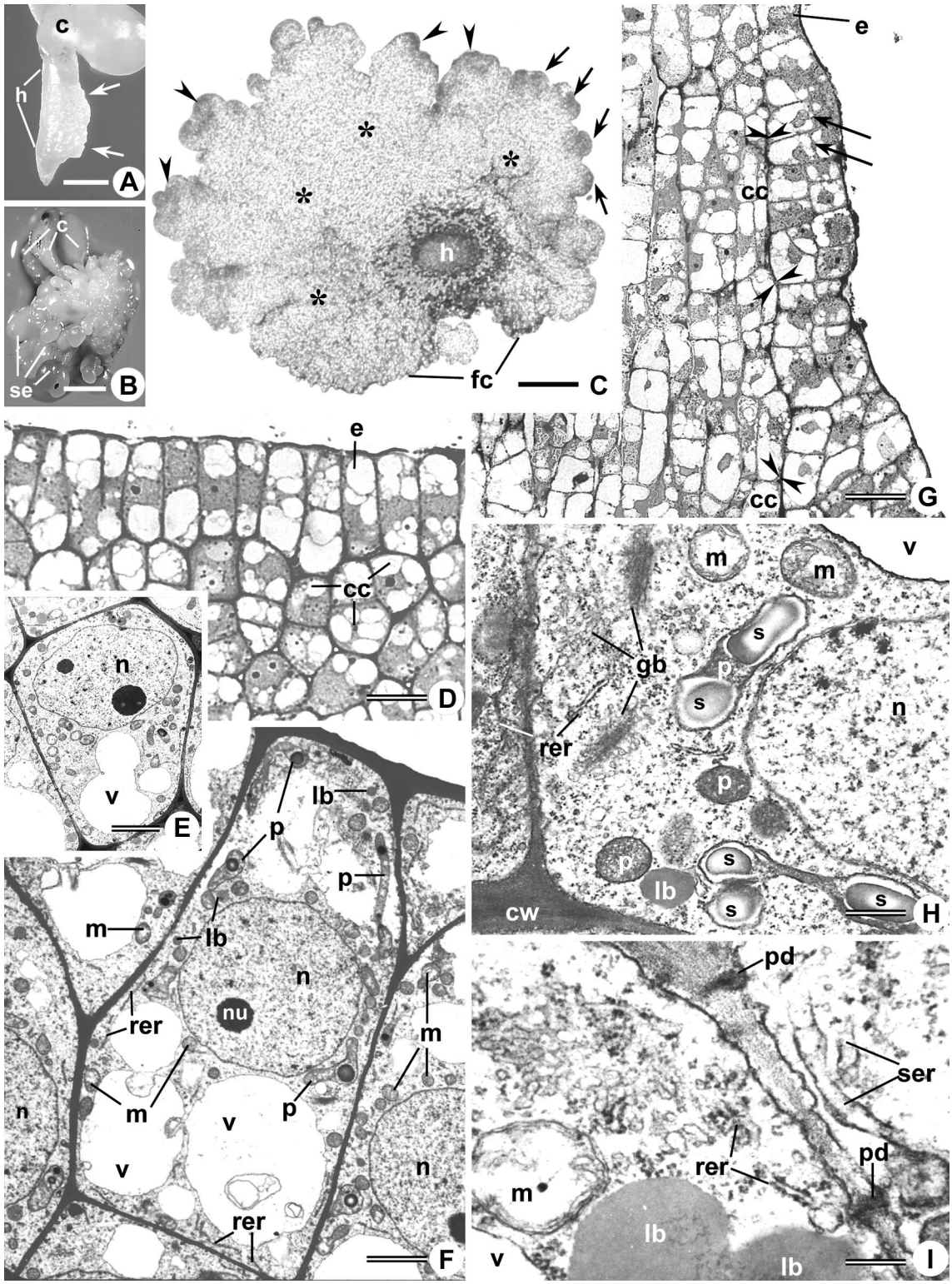

subcellular changes during the developmental sequence of somatic embryo formation by meristematic budding; and (2) to characterize the different embryonic structures found in friable callus to establish the hypothetical sequence from single cells to globular embryos. Furthermore, both embryogenic pathways are compared in the discussion.

MATERIALS AND METHODS

To study somatic embryo formation by the multicellular pathway, a cork oak recurrent embryogenic line maintained on plant-growth-regulator-free medium was used (Fernández-Guijarro *et al*., 1995). Subculture was carried out by transferring early cotyledonary stage embryos of about 5 mm in length to 60 mm diameter baby-food jars containing 50 ml of culture medium. Macronutrients were those from SH (Schenk and Hildebrandt, 1972) and the other components (micronutrients, vitamins, Fe-EDTA) from MS (Murashige and Skoog, 1962), including 3 % sucrose. The culture medium was solidified with 0·6 % agar (Sigma, type E) and pH adjusted to 5·7 before autoclaving at 121°C for 20 min. The cultures were incubated in a growth chamber at 25 ± 2°C, and a 16 h photoperiod (50 μmol m^{-2} s^{-1}) was provided by cool-white plus Grolux fluorescent lamps. Translucent dicotyledonary embryos showing signs of secondary embryogenesis were picked up during subculture and processed for histological examination. As secondary embryogenesis in cork oak is a process showing great asynchrony, the different developmental stages can be examined simultaneously in the same sample (Fig. 1A).

To study somatic embryo formation from friable callus, fragments of both spontaneously forming and induced proliferating friable callus were used. Proliferating friable callus was induced by transferring sections of friable tissue that broke off from the proliferation masses during subculture manipulations to vessels containing 50 ml liquid culture medium made up of MS, containing 3 % sucrose and 10 μM 2,4-dichlorophenoxyacetic acid (2,4-D). About ten pieces of tissue of up to 5 mm diameter were transferred per vessel and cultured in a rotary shaker (100 rpm) in the dark for 7 d at 25 ± 2°C. After treatment, the tissue pieces were subcultured on growth-regulator-free solid medium in a growth chamber at 25 ± 2°C and a 16 h photoperiod, as usual for the maintenance of cork oak embryogenic lines. After 1 month of culture in solid medium, a highly proliferating callus was obtained from which small portions of tissue were randomly taken with forceps for analysis. Tissue portions were slightly shaken in test tubes filled with liquid medium and 1 ml of the supernatant per tube was collected with a 2 mm-diameter Pasteur pipette and examined.

For light microscopy, samples were fixed in 10 % buffered formalin pH 7·2, dehydrated through an isopropyl alcohol series, and embedded in glycol-methacrylate (GMA). Sections 2–3 μm thick were cut and mounted on glass slides. Sections were stained with the periodic acid-Schiff reaction (PA-S), toluidine blue, or thionin as described in Puigderrajols *et al*. (1996). For transmission electron microscopy (TEM), samples were fixed in vacuum for 72 h at room temperature in 2·5 % glutaraldehyde in 0·1M cacodylate buffer. After washing in 0·1M cacodylate buffer, samples were post-fixed in 1 % osmium tetroxide in the same buffer for 2 h. After fixing, samples were dehydrated in a graded series of acetone and embedded in Spurr medium. Thin sections were stained with uranyl acetate and lead citrate, and observed with a Zeiss 910 electron microscope at 60 kV.

RESULTS

Somatic embryo formation by meristematic budding

In our cork oak recurrent system, secondary embryo formation by meristematic budding began by cell divisions at the outer cell layers of the hypocotyl, which led to the formation of a compact mass of proliferation. The newly formed compact mass developed and became convoluted while, at the same time, proliferation extended to neighbouring areas until most of the embryo body was covered. Eventually meristematic budding took place at the periphery of the compact mass, giving rise to secondary embryo formation (Fig. 1A-C; see also Puigderrajols *et al*., 1996).

Commonly, the first visible sign of proliferation was a slight thickening of an area at the apical portion of the hypocotyl observed when the mother embryos were at a very early cotyledonary stage (Fig. 1A). At this stage, the outer cell layers of the hypocotyl consisted of a single-layered epidermis of radially oriented cells, and subjacent cortical cell layers of longitudinal oriented cells (Fig. 1D). Except for shape and orientation, epidermal and cortical cells do not differ greatly. Both contained a large nucleus with a prominent nucleolus and a fragmented vacuole (Fig. 1E and F). Mitochondria were abundant, and long profiles of rough endoplasmic reticulum (ER) appeared adjacent to the cell wall. A few lipid bodies were scattered in the cytoplasm. Plastids showed a scarcely developed inner membrane and very small starch grains. Divisions that led to the formation

FIG. 1. Somatic embryo formation by the multicellular pathway. Early formation of the compact mass. A, Somatic embryo at early cotyledonary stage showing signs of compact mass of proliferation (arrows) at the hypocotyl. Bar = 1 mm. B, Translucent secondary embryos covering most of the hypocotyl of the mother embryo. Bar = 5 mm. C, Cross-section at the hypocotyl showing meristematic primordia (arrows) and developing secondary embryos (arrowheads) at the periphery of the convoluted compact mass (asterisks). The presence of some brownish friable callus is shown. Bar = 1 mm. D, Cross-section of A showing a single-layered epidermis of radially oriented cells and the subjacent cortical cells longitudinally oriented. Bar = 10 μm. E and F, Fine structure of epidermal (F) and cortical (E) cells. Cells show a fragmented vacuole and scarcely developed plastids filled with very small starch grains. Bars = 2 μm. G, Longitudinal section of A showing divisions at the outer cell layers of the hypocotyl. A greater thickness in the cell walls (arrowheads) distinguishes epidermal and cortical derivatives. The first periclinal divisions at the epidermal cell layer are shown (arrows). Bar = 15 μm. H and I, Fine structure of early proliferating epidermal cells. Lipid bodies increase in size and number and dumbbell-shaped plastids are filled with starch grains. Plasmodesmata associated with endoplasmic reticulum are present in the cell walls. Bars = 0·5 μm (H) and 200 nm (I). c, Cotyledon; cc, cortical cells; cw, cell wall; e, epidermis; fc, friable callus; gb, Golgi body; h, hypocotyl; lb, lipid body; m, mitochondria; n, nucleus; nu, nucleolus; p, plastid; pd, plasmodesmata; rer, rough endoplasmic reticulum; s, starch; se, secondary embryos; ser, smooth endoplasmic reticulum; v, vacuole.

of the compact mass occurred at the epidermal cell layer. The plane of the first division was always periclinal and was followed by successive random oriented divisions (Fig. 1G). Although some periclinal and randomly oriented divisions could also be observed at the cortical cell layers, cortical derivatives do not seem to have contributed to the initial proliferating cell mass. At this early stage, cortical derivatives remained distinct from epidermal derivatives and could be recognized by cell orientation and by a perceptibly greater thickness in the cell walls between the two groups.

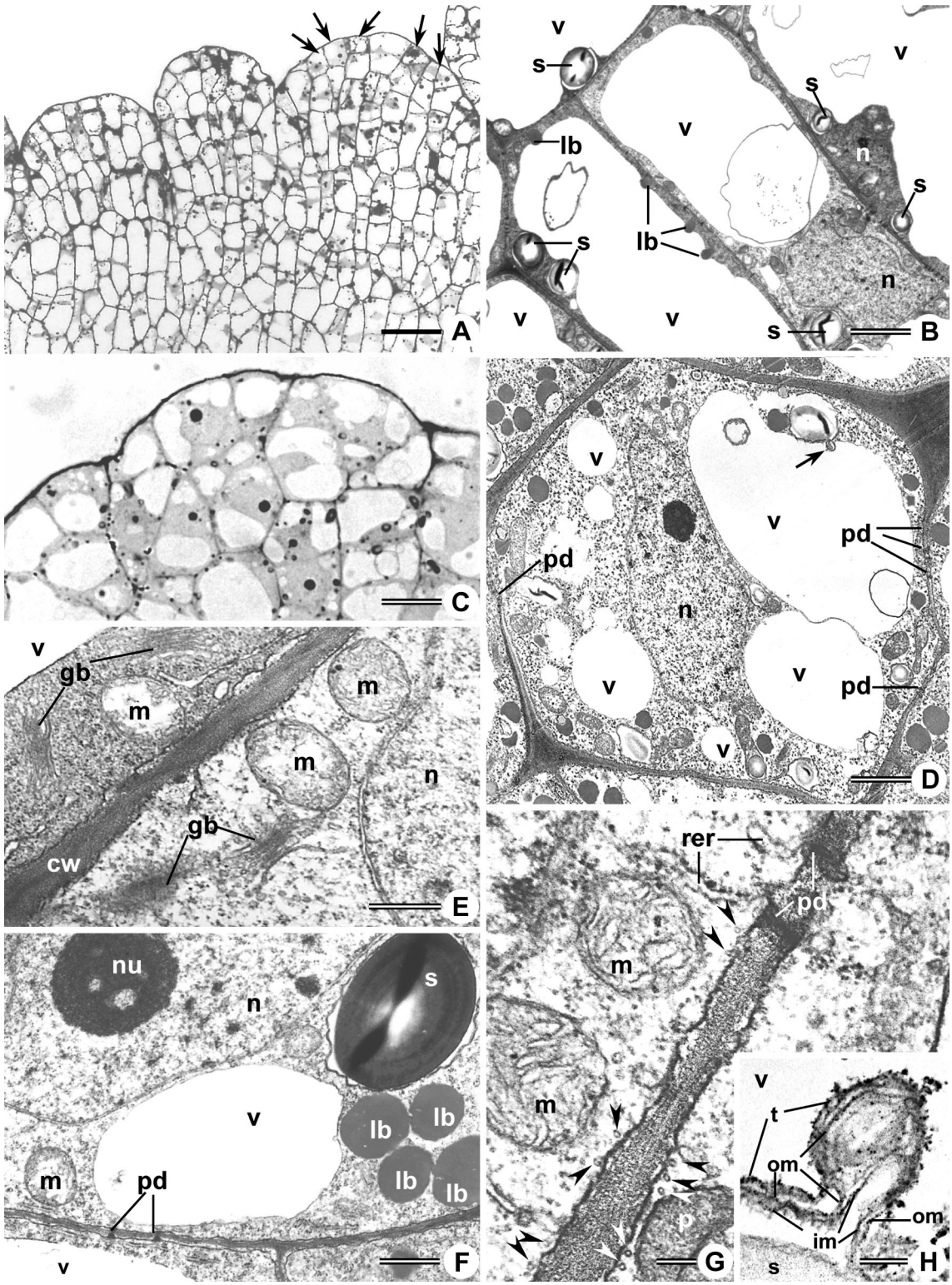

Further divisions of epidermal cells led to a reduction in cell size and cells becoming rounder. The cytoplasm showed an increase in Golgi bodies and rough ER in both short and long profiles. However, in these proliferating cells lipid bodies increased in size and number, and plastids had larger starch grains and took on a dumbbell shape (Fig. 1H). Plasmodesmata associated with smooth ER were present between proliferating cells (Fig. 1I).

Once division started, the proliferating compact mass developed very quickly and soon became convoluted. Eventually, discrete lobes were recognized at its periphery (Fig. 2A). During this evolution of the compact mass, cells enlarged and differentiated and a certain degree of tissue organization was reached (Fig. 2B). Cells in the lobes were filled by a large vacuole and showed a radial orientation. A high accumulation of storage products was noted through the presence of numerous lipid bodies and of plastids largely filled with starch. Between the cells, some plasmodesmatal connections could be observed.

The transition from the compact mass to meristematic primordia occurred at the periphery of the lobes. First, some cells in the outermost cell layer increased their nucleus/cytoplasm ratio and became more isodiametric (Fig. 2A); then, changes extended immediately to other cells located inside (Fig. 2C). Next, meristematic activity was observed through the presence of numerous mitotic figures and, finally, meristematic primordia could be recognized at the periphery of the lobed mass (Fig. 3A). In cells modifying during transition, the vacuole appeared fragmented (Fig. 2D) and the cytoplasm become denser through an increase in free ribosomes. Mitochondria and Golgi bodies were abundant (Fig. 2E) and numerous microtubules were seen lying parallel to the cell wall (Fig. 2G). Wide plasmodesmata with associated ER were highly visible. Although, in general, lipid bodies and starch-containing plastids remained numerous (Fig. 2F), an apparent extrusion of the plastid content to the vacuole could be observed in some cells (Fig. 2D). Plastids located adjacent to the vacuole showed evaginated vesicles encircled by the inner and outer plastid membranes and by the tonoplast (Fig. 2H). When the transition to meristematic primordia was achieved, cells forming the primordia were outlined by thin walls without intercellular spaces (Fig. 3B). In these typically meristematic cells, a dramatic decrease in storage products was detected. Lipid bodies became very scarce and plastids, although present in large numbers, appeared devoid of starch and distorted in shape (Fig. 3C). Most primordia cells had multivesicular bodies (MVB), either free inside the vacuole or related to the tonoplast (Fig. 3B). These MVB consisted of small electron-dense vesicles encircled by a two-membrane system (Fig. 3D).

The differentiation from meristematic primordia to globular embryos was recognized by the organization of a single-layered protodermis and of two internal centres (Fig. 3E and F). Cells in the globular embryo underwent a marked increase in lipid bodies, and plastids became more regular in shape and showed small starch grains (Fig. 3H). Although in these cells a high nucleus/cytoplasm ratio was maintained, the vacuole appeared variable. Possibly related to cell vacuolization, organelle-free cytoplasm areas surrounded by small vacuoles were frequent (Fig. 3G).

Somatic embryogenesis from friable callus

In our cork oak system, a brownish friable callus formed sporadically at the hypocotyl of the mother embryo (see Puigderrajols *et al.*, 1996). Microscopic examination of this brownish callus showed mostly fragments of necrotic tissue in which isolated, cytoplasm-rich isodiametric cells and few-celled aggregates were recognized (Figs 1C, 4A). In addition, an embryogenic friable callus was induced from tissue fragments detached during subculture (see Materials and Methods). The induced callus was yellowish-white in colour, crumbly in appearance and produced somatic embryos that could be isolated easily (Fig. 4B). Under the microscope, the induced callus showed a variety of structures that could be classified in three groups: fragments of non-proliferating tissue with an irregular shape consisting of highly vacuolated cells bearing isolated isodiametric cytoplasm-rich cells and few-celled aggregates mainly at their periphery (Fig. 4C); clusters of meristematic cells, varying in size and shape (Fig. 5A and E); and embryo structures at different stages of development (Fig. 5H and K).

At the ultrastructural level, the isolated isodiametric cytoplasm-rich single cells, about 20 μm in diameter, were characterized by a thick wall, dense cytoplasm, a large nucleus and a large vacuole filled with a fine granular content (Fig. 4D). Plastids were numerous and contained osmiophilic granules and from one to many large starch grains. A large number of lipid bodies was also present. Numerous free ribosomes and rough ER profiles were scattered throughout the cytoplasm (Fig. 4E). The isolated few-celled aggregates consisted of small clusters and narrow strands of cells, usually of two to five cells per section, surrounded by an external cell wall thicker than the internal walls (Fig. 4F). In comparison with single

FIG. 2. Somatic embryo formation by the multicellular pathway. Growth and convolution of the compact mass. Early transition to meristematic primordia. A, Histological section at the periphery of the lobed compact mass showing a radial cell orientation and a conspicuous presence of starch grains. Some more isodiametric cells at the outermost cell layer are shown (arrows). Bar = 50 μm. B, Detail of cells in A showing large vacuoles and abundance of large starch grains and lipid bodies. Bar = 5 μm. C, Histological section at periphery of a lobe at the early transition to meristematic primordia. At this stage, cells show a more isodiametric shape and conspicuous starch grains. Bar = 10 μm. D and H, Fine structure of cells in C. A general view is shown in D and details at higher magnification in E–H. Vacuoles become more fragmented (D); mitochondria and Golgi bodies increase in number (E); lipid bodies and starch grains are still present (F); wide open plasmodesmata and a well-developed cytoskeleton (arrowheads) are commonly seen (G). At this stage, plastids adjacent to the vacuole form extrusions (D, arrow) that consist of (H) the tonoplast and the outer plastid membrane surrounding small vesicles encircled by the inner plastid membrane. Bars = 1·5 μm (D), 0·5 μm (E) 1 μm (F), 0·2·μm (G) and 0·1 μm (H). cw, Cell wall; gb, Golgi body; im, inner plastid membrane; lb, lipid body; m, mitochondria; n, nucleus; nu, nucleolus; om, outer plastid membrane; pd, plasmodesmata; rer, rough endoplasmic reticulum; s, starch; t, tonoplast; v, vacuole.

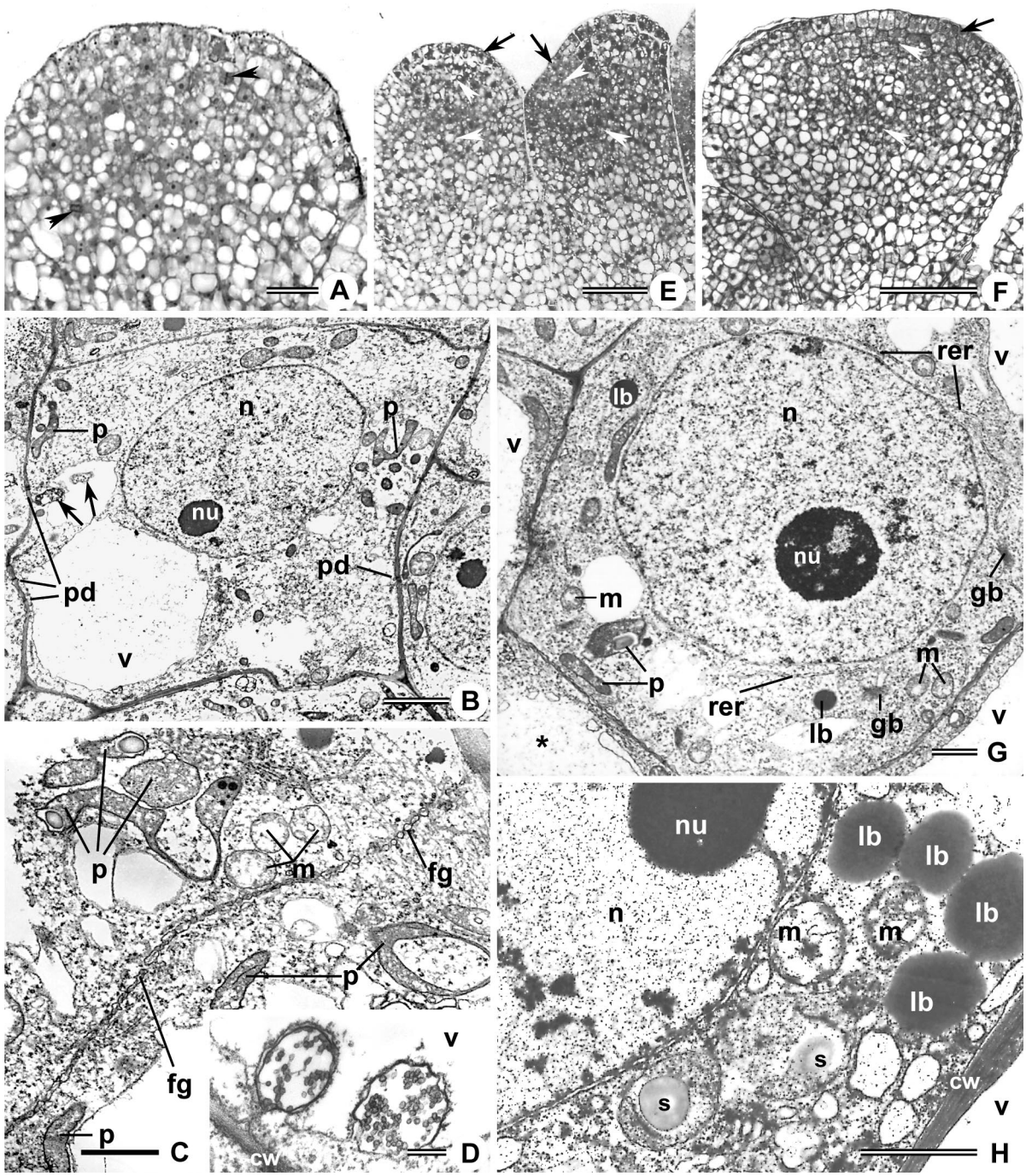

FIG. 3. Somatic embryo formation by the multicellular pathway. Late transition to meristematic primordia and globular stage embryos. A, Histological section of a meristematic primordium showing mitotic figures (arrowheads). Bar = 50 μm. B–D, Fine structure of meristematic cells in A. Nucleus/cytoplasm ratio is high and cell walls thin and without intercellular spaces (B). Very few small lipid bodies and plastids largely devoid of starch and with a distorted shape are observed (C). Multivesicular bodies are commonly seen (B, arrows), related to the tonoplast or free in the vacuole, and consist of a two-membrane system surrounding small vesicles (D). Bars = 5 μm (B), 1 μm (C) and 250 nm (D). E and F, Histological sections of three different stages of globular embryo differentiation from meristematic primordia showing the progressive appearance of the protodermis (arrows) and the two internal organization centers (arrowheads). Bars = 150 μm. G and H, Details of globular embryo cells showing an increase in lipid and starch content and organelle free cytoplasm areas encircled by small vacuoles (asterisk). Bars = 1 μm. cw, Cell wall; fg, fragmoplast; gb, Golgi body; lb, lipid body; m, mitochondria; n, nucleus; nu, nucleolus; p, plastid; pd, plasmodesmata; rer, rough endoplasmic reticulum; s, starch; v, vacuole.

cells, cells in the few-celled aggregates usually had a more fragmented vacuole and a lower number of lipid bodies and, although plastids were equally abundant, starch grains were smaller. All cells in a cluster were connected by numerous plasmodesmata (Fig. 4G), but no plasmodesmata could be found in the external cell wall.

The group of meristematic cell clusters was composed of clumps of small densely packed cytoplasm-rich cells, varying in size and shape. Most cell clusters were free or with attached small remains of non-proliferating tissue. Some of them, usually those of smaller size (about 100 to 200 μm in diameter), were also located at the periphery of non-proliferating tissue fragments (Fig. 4C). Some clusters were globular in shape (Fig. 5A), but other more irregular clusters showed signs of tissue disorganization (Fig. 5E). Small globular-shaped clusters consisted of typically meristematic cells with a high nucleus/cytoplasm ratio, a thin cell wall and dense cytoplasm with numerous free ribosomes (Fig. 5B). Lipid bodies were low in number, and plastids, distorted in shape, were largely devoid of starch. Plastid extrusions and MVBs were related to the vacuole (Fig. 5C and D). All cells in a cluster were connected by plasmodesmata. These small globular clusters had numerous mitotic figures, had no polarity and were unorganized. In contrast, larger globular clusters (about 200 to 400 μm) usually had a shape polarized by the presence of two histological regions with a gradual transition between them. While one region was characterized by small cytoplasm-rich cells, the opposite region had somewhat larger and more vacuolated cells. The more irregularly-shaped clusters (Fig. 5E) were usually also large (up to 500 μm) and had vacuolated cells mainly at their periphery. These vacuolated cells of variable shape showed signs of cell degradation; electron dense accumulations and multilamellar or myelin-like bodies were common between the cell wall and the plasmalemma (Fig. 5F and G).

Globular-shaped embryos were recognized by their well-defined protodermis and signs of internal organization (Fig. 5H). Embryo cells commonly showed a high nucleus/cytoplasm ratio and thin cell walls but their vacuolation was variable. Lipid bodies and plastids with small starch grains were relatively abundant (Fig. 5J). Cytoplasm areas without organelles, encircled by small vacuoles, were commonly seen (Fig. 5I). No intercellular spaces were seen between the cells. When present, embryo structures corresponding to heart-shaped or early cotyledonary stage embryos were free, even though some friable tissue occasionally remained attached (Fig. 5K).

DISCUSSION

Somatic embryogenesis by the multicellular pathway

Results showed that in the cork oak system the compact mass of proliferation is of epidermal origin, although a contribution from the outermost cortical cell layers of the hypocotyl cannot be discounted. The ultrastructural observations about the meristematic budding described above reveal a sequence of cellular changes affecting the symmetry of cell division, cell orientation, organelle composition and the accumulation of storage products. A critical point in this developmental sequence occurs at the periphery of the lobes, when the transition to meristematic primordia begins. Before this point, cells showed a progressive reduction in the nucleus/cytoplasm ratio and a marked increase in storage products (starch grains and lipid bodies). After this point, the nucleus/cytoplasm ratio increased and a progressive reduction in storage products was observed. Changes in the pattern of storage product metabolism and an enhancement of mitotic activity are features commonly associated with the initiation of embryo differentiation (Yeung, 1995). Therefore, the onset of embryo differentiation in the cork oak system seems to be found at this critical point when several neighbouring cells act in a co-ordinated fashion to give rise to meristematic primordia. The multicellular character of this embryogenic pathway is supported by the presence during transition of wide-open plasmodesmata and a well-developed cytoskeleton. Plasmodesmata are recognized as key regulatory elements in cells co-operating as a functional unit (van Bel and van Kesteren, 1999). Cytoskeletal elements are also considered critical for the establishment of embryo polarity (Webb and Gunning, 1991). Therefore, in cork oak the individual meristematic primordia should be considered as pro-embryo structures that precede globular embryo organization.

In pearl millet (Taylor and Vasil, 1996) and in pineapple guava (Canhoto *et al*., 1996), zygotic embryos (primary somatic embryos of multiple-cell origin) differentiate from a meristematic proliferation of epidermal and subepidermal origin after the inductive treatment. In cork oak, somatic cotyledons detached from the embryo axis (Puigderrajols *et al*., 2000), secondary embryos of multicellular origin also differentiated from a meristematic proliferation of parenchyma origin at the petiole. In all these cases, a rapid cell dedifferentiation and a drastic reduction in storage products took place when meristematic proliferation started. According to Taylor and Vasil (1996), embryo development in pearl millet actually begins when epidermal and subepidermal cell dedifferentiation starts and the entire meristematic proliferation is a proembryonal complex. The compact mass to meristematic primordia transition observed in the cork oak recurrent system would be equivalent to this.

Although in cork oak a compact mass of proliferation precedes secondary embryo formation, this compact mass should not be considered as a true callus. The compact mass shows a certain degree of tissue organization and it is unable to proliferate indefinitely as usually occurs in callus proliferations. Therefore, cells in the compact mass should be seen as pre-embryogenically determined cells (PEDC) from which embryo differentiation proceeds without a prior redetermination phase. Therefore, secondary embryogenesis in cork oak should be considered direct, at least in the sense that no undifferentiated callus phase is present before embryogenic cell determination (Sharp *et al*., 1980). However, some authors (Duhem *et al*., 1989) suggest that the presence of such limited proliferation before embryogenesis would be an intermediate modality between direct and indirect embryogenesis.

Somatic embryogenesis by the unicellular pathway

Although ours was not a sequential analysis, from the comparison of the different structures found in cork oak friable callus with the structures described in the literature for other friable systems, a hypothetical development

sequence from single cells to globular embryos may be proposed in which the isolated few-celled aggregates and the clusters of meristematic cells may represent intermediate stages.

Isodiametric cytoplasm-rich single cells in cork oak have the same features as embryogenic cells in other systems, such as carrot (Halperin and Jensen, 1967), guinea grass (Karlsson and Vasil, 1986), maize (Fransz and Schel,

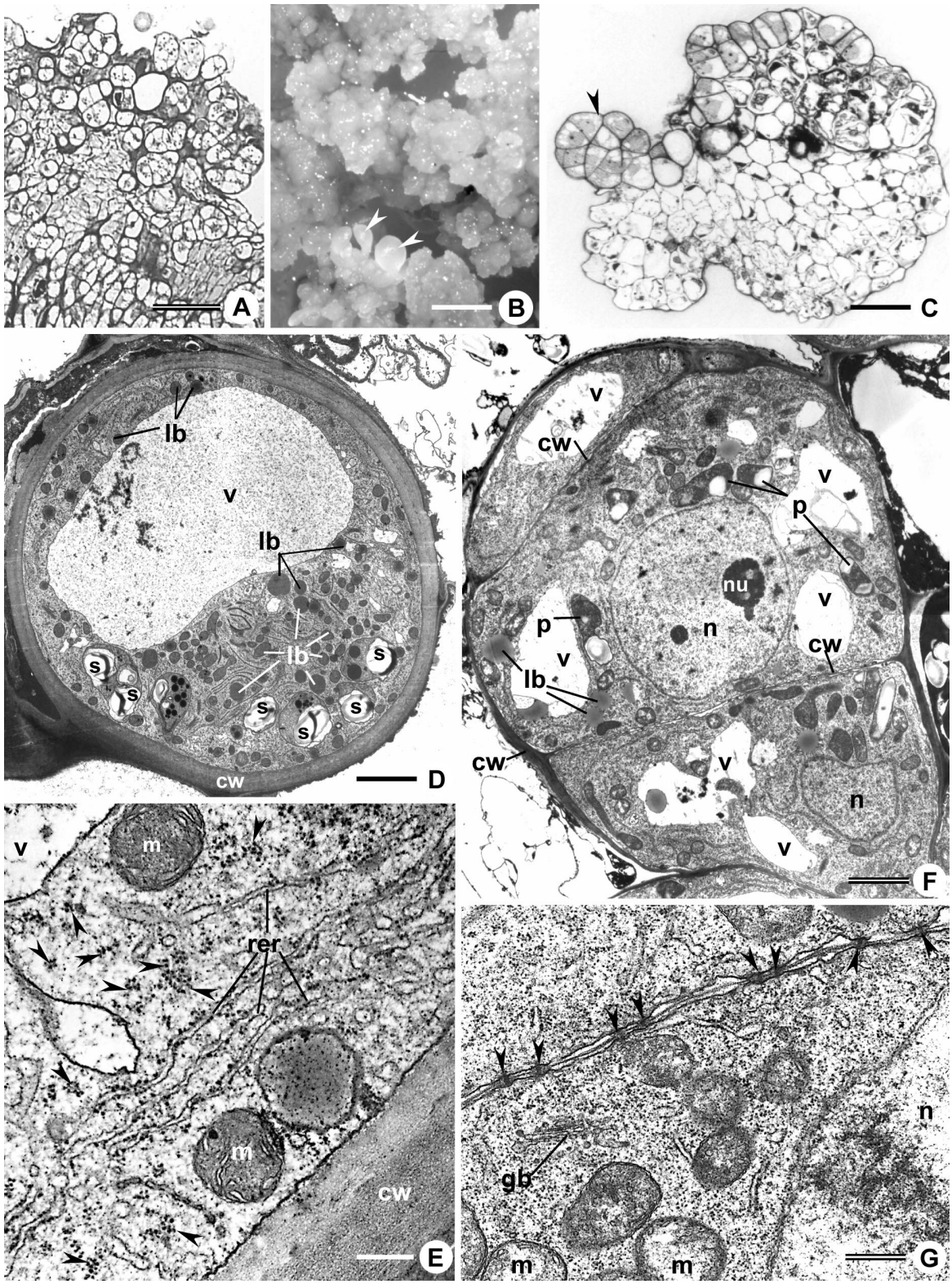

1991*a*) or pearl millet (Taylor and Vasil, 1996). The most outstanding features of these cells are a high nucleus/cytoplasm ratio, dense cytoplasm and the presence of large amounts of lipids and starch. It is reported in the literature that single cells divide to form few-celled proembryo structures which are referred to as proembryo-like units in carrot (Halperin and Jensen, 1967), embryogenic units in maize (Fransz and Schel, 1991*a*) or proembryonic cell masses in pearl millet (Taylor and Vasil, 1996). Such proembryo structures correspond to the isolated few-celled aggregates in cork oak. The presence of a thick cell wall surrounding these aggregates, which probably represents the wall of the original single cell, supports this hypothesis (Vasil and Vasil, 1982*b*; Karlsson and Vasil, 1986). The absence of plasmodesmata in the external cell wall and their presence in the internal walls reinforce this view. The globular clusters of meristematic cells represent proembryo structures derived from few-celled aggregates. Small globular clusters without visible polarity correspond to earlier proembryos, whereas globular clusters in which polarity has been already established correspond to later stages before globular embryo differentiation. In carrot suspension cultures, few-celled proembryo structures increase their division rate, which leads to the formation of dense globular cell masses that, according to Halperin and Jensen (1967), are functional proembryos. Maize proembryonic structures, referred to as embryogenic units, evolve to somatic embryos through intermediate structures, referred to as transition units (Fransz and Schel, 1991*a*, *b*). These maize transition units would correspond to the cork oak polarized globular meristematic cell clusters.

A relatively high rate of proliferation characterizes the induced friable callus in cork oak. This proliferating capacity could be related to alternating cycles of growth and fragmentation. The tissue disorganization shown by the clusters with a more irregular shape provides evidence of such behaviour. Some cells in these more irregular clusters show signs of degradation, such as the presence of multilamellar bodies (Konar *et al*., 1972; Verdus *et al*., 1993) and electron dense accumulations (Rohr *et al*., 1989). Cell degradation may lead to tissue fragmentation, followed by a reinitiation of the growing cycle. Such behaviour may represent a failure in proembryo development as a result of inadequate culture conditions. According to Sachs (1991), a weak signal that destabilizes polarity may inhibit further proembryo development. Thus, culture conditions play an important role in the establishment and maintenance of embryo polarity. Under the continued presence of auxin, proembryogenic cell masses in carrot suspension culture undergo cycles of growth and fragmentation but, on low or no auxin, embryo development proceeds rapidly from small proembryogenic cell masses (Halperin, 1995).

Storage products and embryogenesis

There is a general consensus that reserves are crucial to morphogenetic processes. The presence of high levels of hydrocarbon reserves such as starch has been reported at the beginning of several *in vitro* development processes (Mangat *et al*., 1990; Branca *et al*., 1994). In addition, a dramatic decrease in starch amounts has been reported when organogenesis and somatic embryogenesis start (Mangat *et al*., 1990; Martin *et al*., 2000). Our observations of cork oak corroborate these earlier findings. In the meristematic budding pathway, the highest levels in lipid and starch content are reached in the compact mass cells before primordia initiation. The highest levels of reserves in the friable callus pathway are shown by isodiametric cytoplasm-rich single cells. However, the minimum levels correspond to cells in meristematic primordia and in the small clusters of meristematic cells. Therefore, in both pathways, a change in the pattern of storage product metabolism occurs at the moment at which somatic embryo differentiation apparently begins. It is known that sucrose has a significant regulatory and integrative function in plant development and that changes in sucrose content are transduced into changes in gene expression (Farrar *et al*., 2000). It is very possible that the rapid hydrolysis of starch when embryogenesis starts provides not only energy and carbon sources for proliferation, but may also play a regulatory role.

Our results suggest a possible role for MVB in the rapid catabolism of starch. In fact, one of the most outstanding features in the modifying cells during compact mass-to-meristematic primordia transition was the apparent extrusion of the plastid content into vacuole, followed by an increase in MVB, either free or related to the tonoplast. Moreover, in friable callus, plastid extrusions and MVB were very abundant in the small globular clusters of meristematic cells. Although MVB have been reported in embryogenic systems, their origin has been commonly related to ER or Golgi apparatus (Verdus *et al*., 1993). That MVB may also originate in plastids is supported by ultrastructural observations of the membrane system involved in plastid extrusions and the morphology of MBV in our cork oak system.

The results presented in this paper confirm the hypothesis of Williams and Maheswaran (1986) that single-cell and

FIG. 4. Somatic embryo formation from friable callus. Isolated single cells and few-celled aggregates. A, Histological section of friable callus showing isolated single cells and few-celled aggregates (see also Fig. 1C). Bar = 75 μm. B, Morphological view of induced friable callus showing a crumbly appearance and the presence of early cotyledonary stage embryos (arrowheads). Bar = 5 mm. C, Histological section of an irregularly shaped fragment of tissue in B, showing isolated cells and few-celled aggregates at the periphery. A small globular cluster of meristematic cells is also shown (arrowhead). Bar = 50 μm. D and E, Fine structure of the single-isodiametric cells. In a general view (D), the thick cell wall and the high presence of lipid bodies and starch-containing plastids with osmiophilic granules are shown. Abundant free ribosomes (arrowheads) and rough ER profiles are seen at higher magnification (E). Bars = 3 μm (D) and 250 nm (E). F and G, Fine structure of the few-celled aggregates. F, General view of a narrow strand of cells showing the outer cell wall thicker than the internal walls, a more fragmented vacuole, a low number of lipid bodies and plastids with smaller starch grains. Bar = 5 μm. G, Higher magnification of F showing an internal cell wall with numerous plasmodesmata connections (arrowheads). Bar = 500 nm. cw, Cell wall; lb, lipid body; m, mitochondria; n, nucleus; nu, nucleolus; p, plastid; rer, rough endoplasmic reticulum; s, starch; v, vacuole.

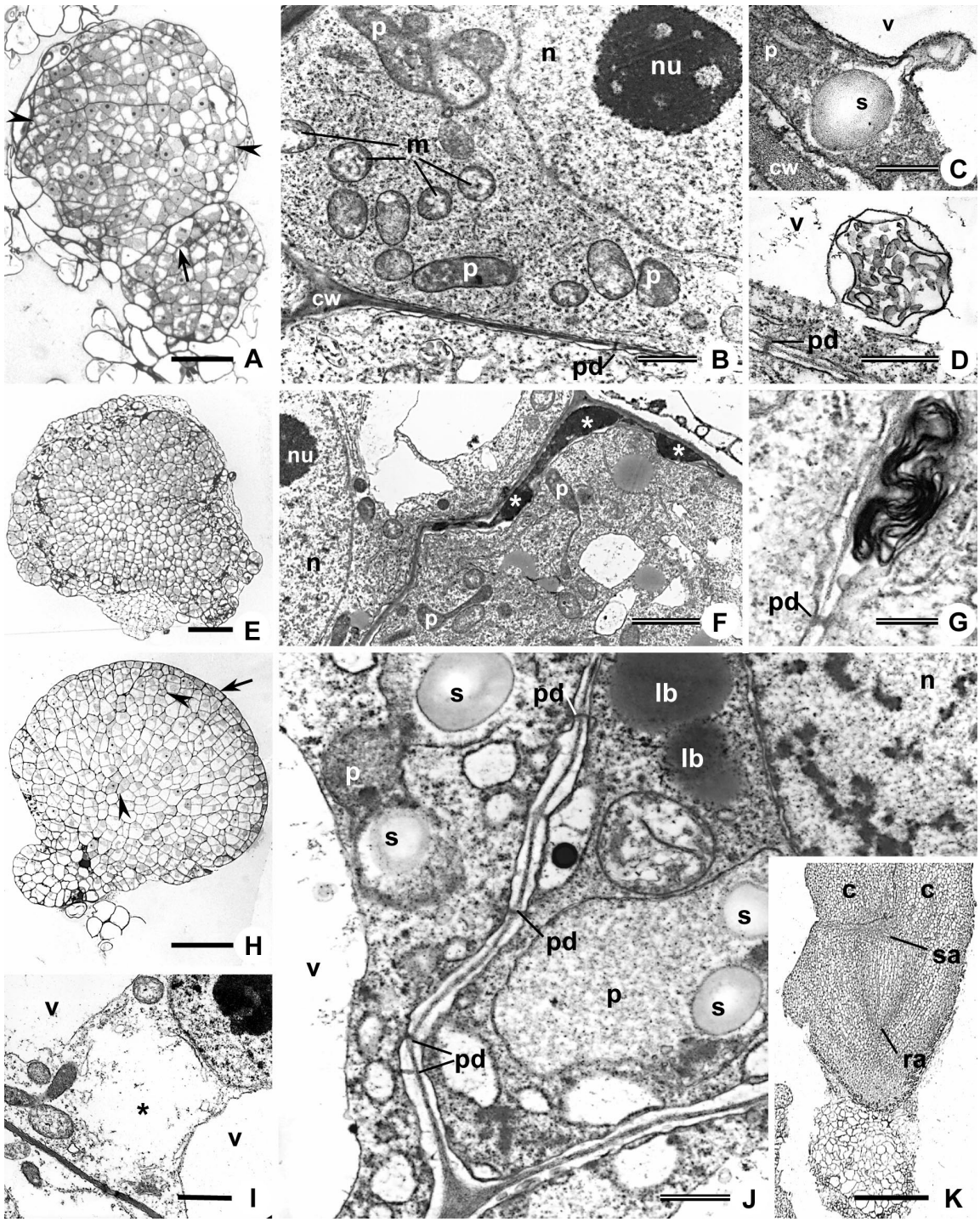

FIG. 5. Somatic embryo formation from friable callus. Clusters of meristematic cells and somatic embryo structures. A, Histological section of two adjacent globular-shaped clusters of meristematic cells. Mitosis (arrow) is shown in the smaller cluster of cells, as the larger is characterized by the presence of two opposed histological regions (arrowheads). Bar = 80 μm. B, Fine structure of meristematic cells in globular-shaped clusters. Cells show thin cell walls, abundant free ribosomes and plastids devoid of starch and distorted in shape (B). Plastid extrusions (C) and multivesicular bodies (D) are related to the vacuole. Bars = 75 μm (B), 250 nm (C) and 500 nm (D). E, Histological section of a larger globular-shaped cluster of meristematic cells with a more irregular shape and showing signs of tissue disorganization at their periphery. Bar = 100 μm. F and G, Fine structure of more vacuolated cells at the periphery of E showing electrodense accumulations (asterisks) (F) and multilamellar or myelin-like bodies (G) between cell walls and the plasmalemma. Bars = 2 μm (F) and 250 nm (G). H, Histological section of an isolated globular embryo structure showing a well defined protodermis (arrow) and two organization centres (arrowheads). Bar = 100 μm. I and J, Fine structure of globular embryo cells showing organelle-free-cytoplasm area (asterisk) encircled by small vacuoles (I) and the presence of lipid bodies and plastids with small starch grains (J). Bars = 1 μm (I) and 500 nm (J). K, Longitudinal section of an early cotyledonary stage somatic embryo attached to a remainder of friable tissue. Bar = 1 mm. c, Cotyledon; cw, cell wall; lb, lipid body; m, mitochondria; n, nucleus; nu, nucleolus; p, plastid; pd, plasmodesmata; s, starch; sa, shoot apex; ra, root apex; v, vacuole.

multiple-cell embryogenic pathways are different forms of the same general process and that, in both, cellular changes follow a similar sequential pattern. Further investigation into the cork oak system should be centred on the study of culture conditions which allow high rates of embryo development from single cells.

ACKNOWLEDGEMENTS

We thank Mr Mariano Toribio and Mrs Cristina Celestino (IMIA, Instituto Madrileño de Investigaciones Agrarias y Alimentarias). This research was supported by DGES project PB96–0450-A.

LITERATURE CITED

Branca C, Torelli A, Fermi P, Altamura MM, Bassi M. 1994. Early phases '*in vitro*' culture tomato cotyledons: starch accumulation and protein pattern in relation to the hormonal treatment. *Protoplasma* **182**: 59–64.

Canhoto JM, Mesquita JF, Cruz GS. 1996. Ultrastructural changes in cotyledons of pineapple guava (Myrtaceae) during somatic embryogenesis. *Annals of Botany* **78**: 513–521.

Duhem K, Le Mercier N, Boxus P. 1989. Donnés nouvelles sur l'induction et le dévelopment d'embryons somatiques chez *Theobroma cacao* L. *Café Cacao Thé* **33**: 9–14.

Farrar J, Pollock C, Gallagher J. 2000. Sucrose and the integration of metabolism in vascular plants. *Plant Science* **154**: 1–11.

Fernández-Guijarro B, Celestino C, Toribio M. 1995. Influence of external factors on secondary embryogenesis and germination in somatic embryos from leaves of *Quercus suber* L. *Plant Cell Tissue and Organ Culture* **41**: 99–106.

Fransz PF, Schel JHN. 1991*a*. Cytodifferentiation during the development of friable embryogenic callus of maize (*Zea mays*). *Canadian Journal of Botany* **69**: 26–33.

Fransz PF, Schel JHN. 1991*b*. An ultrastructural study on the early development of *Zea mays* somatic embryos. *Canadian Journal of Botany* **69**: 858–865.

Fransz PF, Schel JHN. 1994. Ultrastructural studies on callus development and somatic embryogenesis in *Zea mays* L. In: Bajaj YPS, ed. *Biotechnology in agriculture and forestry vol. 25, Maize*. Berlin: Springer-Verlag, 50–65.

Halperin W. 1995. *In vitro* embryogenesis: Some historical issues and unresolved problems. In: Thorpe TA, ed. *In vitro embryogenesis in plants*. Dordrecht: Kluwer Academic Publishers, 1–16.

Halperin W, Jensen WA. 1967. Ultrastructural changes during growth and embryogenesis in carrot cell cultures. *Journal of Ultrastructure Research* **18**: 428–443.

Hepher A, Boulter ME, Harris N, Nelson RS. 1988. Development of a superficial meristem during somatic embryogenesis from immature cotyledons of soybean (*Glycine max L.*). *Annals of Botany* **62**: 513–519.

Karlsson SB, Vasil IK. 1986. Morphology and ultrastructure of embryogenic cell suspension cultures of *Panicum maximum* (Guinea grass) and *Pennisetum purpureum* (Napier grass). *American Journal of Botany* **73**: 894–901.

Konar RN, Thomas E, Street HE. 1972. Origin and structure of embryoids arising from epidermal cells of the stem of *Ranunculus sceleratus* L. *Journal of Cell Science* **11**: 77–93.

McCain JW, Hodges TK. 1986. Anatomy of somatic embryos from maize embryo cultures. *Botanical Gazette* **147**: 453–460.

Mangat BS, Pelekis MK, Cassells AC. 1990. Changes in the starch content during organogenesis in '*in vitro*' cultured *Begonia rex* stem explants. *Physiologia Plantarum* **79**: 267–274.

Martin AB, Cuadrado Y, Guerra H, Gallego P, Hita O, Martin L, Dorado A, Villalobos N. 2000. Differences in the contents of total sugars, reducing sugars, starch and sucrose in embryogenic and non-embryogenic calli from *Medicago arborea* L. *Plant Science* **154**: 143–151.

Merkle SA. 1995. Strategies for dealing with limitations of somatic embryogenesis in hardwood trees. *Plant Tissue Culture Biotechnology* **1**: 112–121.

Murashige T, Skoog F. 1962. A revised medium for rapid growth and bio-assays with tobacco tissue cultures. *Physiologia Plantarum* **15**: 473–497.

Puigderrajols P, Fernández-Guijarro B, Toribio M, Molinas M. 1996. Origin and early development of secondary embryos in *Quercus suber* L. *International Journal of Plant Sciences* **157**: 674–684.

Puigderrajols P, Celestino C, Suils M, Toribio M, Molinas M. 2000. Histology of organogenic and embryogenic responses in cotyledons of somatic embryos of *Quercus suber* L. *International Journal of Plant Sciences* **161**: 353–362.

Rohr R, von Aderkas P, Bonga JM. 1989. Ultrastructural changes in haploid embryoids of *Larix decidua* during early embryogenesis. *American Journal of Botany* **76**: 1460–1467.

Sachs T. 1991. *Pattern formation in plant tissues*. Cambridge: Cambridge University Press.

Schenk RU, Hildebrandt AC. 1972. Medium and techniques for induction and growth of monocotyledoneous and dicotyledoneous plant cell cultures. *Canadian Journal of Botany* **50**: 199–204.

Schwendimann J, Pannetier C, Michaux-Ferrière N. 1988. Histology of somatic embryogenesis from leaf explants of the oil palm *Elaeis guineensis*. *Annals of Botany* **62**: 43–52.

Sharp WR, Söndahl MR, Caldas LS, Maraffa SB. 1980. The physiology of *in vitro* sexual embryogenesis. *Horticultural Reviews* **2**: 268–310.

Stamp JA. 1987. Somatic embryogenesis in cassava: the anatomy and morphology of the regeneration process. *Annals of Botany* **59**: 451–459.

Taylor MG, Vasil IK. 1996. The ultrastructure of somatic embryo development in pearl millet (*Pennsisetum glaucum*; Poaceae). *American Journal of Botany* **83**: 28–44.

Toonen MAJ, Hendricks T, Schmidt EDL, Verhoeven HA, van Kammen A, de Vries SC. 1994. Description of somatic-embryo-forming single cells in carrot suspension cultures employing video cell tracking. *Planta* **194**: 565–572.

van Bel AJE, van Kesteren WJP. 1999. *Plasmodesmata: structure, function, role in cell communication*. Berlin: Springer-Verlag.

Vasil V, Vasil IK. 1982. The ontogeny of somatic embryos of *Pennisetum americanum* (L) K. Schum. I. In cultured immature embryos. *Botanical Gazette* **143**: 454–465.

Verdus MC, Dubois T, Dubois J, Vasseur J. 1993. Ultrastructural changes in leaves of *Cichorium* during somatic embryogenesis. *Annals of Botany* **72**: 375–383.

Webb MC, Gunning BES. 1991. The microtubular cystoskelelon during development of the zygote, proembryo and free-nuclear endosperm in *Arabidopsis thaliana* (L.) Heynh. *Planta* **184**: 187.

Wernicke W, Potrykus I, Thomas E. 1982. Morphogenesis from cultured leaf tissue of *Sorghum bicolor*. The morphogenetic pathways. *Protoplasma* **111**: 53–62.

Williams EG, Maheswaran G. 1986. Somatic embryogenesis: Factors influencing coordinated behaviour of cells as an embryogenic group. *Annals of Botany* **57**: 443–462.

Yasuda H, Nakajima M, Masuda J, Ohwada T. 2000. Direct formation of heart-shaped embryos from differentiated single carrot cells in culture. *Plant Science* **152**: 1–6.

Yeung EC. 1995. Structural and developmental patterns in somatic embryogenesis. In: Thorpe TA, ed. In vitro *embryogenesis in plants*. Dordrecht: Kluwer Academic Publishers, 205–247.